Critical role for the NLRP3 inflammasome during acute lung injury[1]

Jamison J. Grailer, **Bethany A. Canning**, **Miriam Kalbitz**, **Mikel D. Haggadone**, **Rasika M. Dhond**, **Anuska V. Andjelkovic**, **Firas S. Zetoune**, and **Peter A. Ward**[*]

Department of Pathology, University of Michigan Medical School, Ann Arbor, MI, 48109 USA

Abstract

The inflammasome is a key factor in innate immunity and senses soluble pathogen and danger associated molecular patterns as well as biological crystals (urate, cholesterol, etc.), resulting in expression of IL-1β and IL-18. Using a standard model of acute lung injury (ALI) in mice featuring airway instillation of LPS, ALI was dependent on availability of NLRP3 as well as caspase-1, which are known features of the NLRP3 inflammasome. The appearance of IL-1β, a product of NLRP3 inflammasome activation, was detected in bronchoalveolar lavage fluids (BALF) in a macrophage- and neutrophil-dependent manner. Neutrophil-derived extracellular histones appeared in the BALF during ALI and directly activated the NLRP3 inflammasome. Antibody-mediated neutralization of histones significantly reduced IL-1β levels in BALF during ALI. Inflammasome activation by extracellular histones in LPS-primed macrophages required NLRP3 and caspase-1 as well as extrusion of K^+, increased $[Ca^{+2}]i$, and generation of reactive oxygen species. NLRP3 and caspase-1 were also required for full extracellular histone presence during ALI, suggesting a positive feedback mechanism. Extracellular histone and IL-1β levels in BALF were also elevated in C5a-induced and IgG immune complex ALI models suggesting a common inflammatory mechanism. These data indicate an interaction between extracellular histones and the NLRP3 inflammasome, resulting in ALI. Such findings suggest novel targets for treatment of ALI, for which there is currently no known efficacious drug.

INTRODUCTION

Acute lung injury (ALI) and acute respiratory distress syndrome (ARDS) often occur in sepsis and in hemorrhagic shock. The annual incidence of ALI/ARDS in the United States approximates 200,000 cases, with estimated mortality rates ranging from 25–60% (1, 2). These conditions are characterized by the accumulation of neutrophils in the lung and the production of inflammatory mediators including complement activation products, cytokines and chemokines, proteases, and oxidants. Vascular endothelial and alveolar epithelial cell damage/death leads to disruption of the blood-alveolar barrier, resulting in pulmonary edema, intrapulmonary hemorrhage, and severely impaired gas exchange (reviewed, 3).

[*]Correspondence to: Dr. Peter A. Ward[2], phone: (734) 647-2921; fax: (734) 764-4308; pward@med.umich.edu.
[2]Correspondence address: Dr. Peter A. Ward, Department of Pathology, University of Michigan Medical School, 1301 Catherine Rd., Ann Arbor, MI 48109, USA

However, the molecular mechanisms responsible for the development of these conditions are poorly understood, and there are currently no FDA-approved drug therapies.

The NLRP3 inflammasome is a major intracellular multi-protein inflammatory pathway of the innate immune system. Upon activation, there ensues activation of caspase-1, the processing of cytokine precursors (pro-IL-1β and pro-IL-18) to their mature biologically active and secreted forms, followed by pyroptosis (4). It is apparent that agonists of TLRs do not directly activate the NLRP3 inflammasome. However, TLR agonism is a prerequisite for optimal activation of the NLRP3 inflammasome, resulting in production of relevant proteins (5). Therefore, activation of the NLRP3 inflammasome requires stimuli that both prime and activate the inflammasome. Activating stimuli for the NLRP3 inflammasome are diverse and include both endogenous factors (ATP, uric acid crystals, etc.) and exogenous factors (bacterial hemolysins, pneumolysin, etc.) (4). The signals from these various stimuli converge on a pathway that involves dysregulated ionic balance (K^+ efflux, elevated intracellular Ca^{+2}), and lysosome and mitochondrial damage, leading to the release of cathepsins and the production of reactive oxygen species (ROS) (4). The requirements for each of these factors in NLRP3 inflammasome activation are stimulus-dependent. The exact mechanism of activation remains intensely debated (6–9). Altogether, activation of the NLRP3 inflammasome requires integrated signals resulting in priming and cellular damage or stress which results in activation.

Despite intense study of the NLRP3 inflammasome function over the last decade, the contribution of the NLRP3 inflammasome to ALI/ARDS remains largely unknown. The products of inflammasome activation (IL-1β and IL-18) play a prominent role in promoting ALI. Elevated levels of IL-18 occur in humans with ARDS and have been associated with a poor long-term prognosis in ALI/ARDS (10, 11). Antibody neutralization of IL-18 reduced lung injury during experimental ALI in mice (10, 12). In addition, antibody neutralization of IL-1β, or administration of IL-1 receptor antagonist (IL-1RA) attenuated ALI severity in several different rodent models (13–15). Importantly, the inflammasome adaptor protein, ASC, appears to be required for lung IL-1β production during bleomycin-induced pulmonary inflammation (16). Also, the NLRP3 inflammasome has been reported to be activated in lung endothelial cells following hemorrhagic shock (17). Evidence has accumulated suggesting that the NLRP3 inflammasome contributes to ventilator-induced acute lung injury and to chronic lung diseases such as asthma and chronic obstructive pulmonary disease (13, 18). Despite the evidence of inflammasome activation products in driving ALI, and the importance of the NLRP3 inflammasome in some models of lung inflammation, the molecular mechanisms required to activate the NLRP3 inflammasome during ALI remain undefined.

Anakinra (Kineret™) is a recombinant human IL-1RA that is FDA-approved for the treatment of rheumatoid arthritis and for a severe form of cryopyrin-associated periodic syndrome (CAPS), termed neonatal-onset multisystem inflammatory disease (NOMID). During bleomycin-induced ALI, administration of anakinra significantly reduced neutrophil infiltration into lung and levels of cytokines/chemokines in bronchoalveolar lavage fluids (BALF) (16). Anakinra may be a useful therapeutic targeting inflammasome activation products during ALI/ARDS. However, there is a paucity of knowledge concerning the role,

source, and mechanism of IL-1β production during ALI, which may preclude current use of anakinra as a therapeutic strategy.

Histones are nuclear proteins that are packaged as octets in coils of DNA and play key roles in regulation of gene transcription. The appearance of extracellular histones has been described during traumatic and shock-associated conditions, with levels in plasma reaching as high as 100 μg/ml following polytrauma in humans (19). Extracellular histones are pro-inflammatory mediators, as shown by the observation that a histone-neutralizing antibody reduced injury and/or enhanced survival in rodent models of sepsis, endotoxemia, and ischemia/reperfusion injury (20–22). We have recently demonstrated the presence of extracellular histones in BALF of mice and humans during ALI (23). Antibody neutralization of histones significantly reduced the level of injury during experimental ALI (23). However, the exact mechanism of histone-induced lung inflammation remains unclear.

In this report, we investigated the role of the NLRP3 inflammasome during ALI and the contribution of extracellular histones to NLRP3 inflammasome activation. The NLRP3 inflammasome and caspase-1 were critical for full development of ALI. Extracellular histones directly activated the NLRP3 inflammasome and induced IL-1β release in a caspase-1-dependent manner. NLRP3 activation resulted in enhanced neutrophil recruitment and robust histone release in vivo, which suggests a positive feedback mechanism between extracellular histones and NLRP3 inflammasome activation. Taken together, we describe a novel mechanism of pulmonary inflammation (ALI) involving the NLRP3 inflammasome and extracellular histones.

MATERIALS AND METHODS

Animals

All procedures were performed within the U.S. National Institutes of Health guidelines and were approved by the University of Michigan Committee on the Use and Care of Animals. Male age-matched C57BL/6 (wild type), NLRP3-deficient (NLRP3$^{-/-}$) (24), and caspase-1$^{-/-}$ (25) (C57BL/6N wild type control) mice were purchased from the Jackson Laboratories (Bar Harbor, ME). All animals were housed under specific pathogen-free conditions with free access to food and water.

Reagents

Mixed calf thymus histones (purified, Type II-A), LPS (*E. coli* o111:B4), ATP, BAPTA-AM, 2-aminoethyl diphenylborinate (2-APB), N-acetyl-L-cysteine (NAC), cytochalasin B, PMA, and BSA were from Sigma (St. Louis, MO). Mixed calf thymus histones were used for all experiments unless otherwise indicated. Histone stocks were dissolved in PBS, pH 7.4, and stored at −80°C until use. The endotoxin level of histone preparations was determined to be < 0.02 EU/mg protein (LAL method; Lonza, Basel, Switzerland). Purified and recombinant individual histones were used for this study: H1 (purified from calf thymus; Roche, Indianapolis, IN), H2A (recombinant; Cayman Chemical, Ann Arbor, MI), H2B (recombinant; Cayman Chemical), H3 (purified from calf thymus, Roche), and H4 (recombinant; Cayman Chemical). Y-VAD-CMK was from Cayman Chemical. Where

indicated, histone preparations were treated with DNase, RNase, or proteinase K (all from Sigma) for 30 min at 37°C, then 75°C for 10 min. Anti-histone H2A/H4 antibody (clone BWA3 (26)) was purified from ascites by protein A/G chromatography. Recombinant mouse C5a was from R & D Systems (Minneapolis, MN).

Acute lung injury

LPS-induced ALI was performed as previously described (27). Briefly, following anesthetization with ketamine, mice received 60 μg of LPS intratracheally (i.t.) during inspiration in a volume of 30 μl saline. Sham control mice received sterile saline. BALF was harvested by the slow instillation and retraction of 1 ml PBS. Neutrophils were counted on a hemocytometer following lysis of erythrocytes. BALF was aliquoted and stored at −80°C until use. In some cases, neutrophils were depleted with anti-Ly6G (clone 1A8, 100 μg/ mouse; BioLegend, San Diego, CA), administered 12 hours prior to ALI. Blood neutrophils were confirmed to be depleted >95%. In some cases, macrophages were depleted with clodronate liposomes (250 μg total clodronate; Encapsula NanoSciences, Nashville, TN) administered i.t. 24 hours prior to ALI. Control mice received an equivalent amount of PBS-filled liposomes. Following clodronate liposome administration, lavagable alveolar macrophages were reduced by >80%. In some cases, anti-histone H2A/H4 (BWA3) was administered during ALI (100 μg i.p. and 50 μg i.t.). Mouse IgG (Jackson Immunoresearch, West Grove, PA) was used as a control antibody. For C5a-induced ALI, 500 ng of recombinant mouse C5a was administered i.t. in 30 μl PBS. Sham mice received sterile PBS. For IgG immune complex-induced ALI, 125 μg of anti-BSA (MP Biomedicals, Solon, OH) was administered i.t. in 40 μl saline followed by i.v. injection of 1 mg BSA in 200 μl sterile saline. Sham mice received anti-BSA i.t. but only saline i.v.

In vitro assays

Mouse bone marrow neutrophils were harvested by flushing bilateral femurs with Hanks' balanced salt solution (Life Technologies, Grand Island, NY). Erythrocytes were lysed in hypotonic buffer. Cells were washed in PBS and layered on Histopaque 1077 (Sigma) for density gradient centrifugation (500 x g, 30 min, 4°C). The pellet (neutrophils) was washed with PBS and cultured in RPMI media (Life Technologies) supplemented with 0.1% BSA. PMN purity was $86 \pm 4\%$ (mean ± SD) and $82 \pm 3\%$ as determined by flow cytometry (Ly6G^{+}CD11b^{+}) and Wright-stained cytospin preparations, respectively.

Mouse peritoneal macrophages were elicited by i.p. injection of 1.5 ml of 2.4% thioglycollate (Life Technologies). Macrophages were harvested 4 days later by i.p. instillation and retraction of 8 ml sterile PBS. Cells were purified by adherence and cultured in RPMI media supplemented with 0.1% BSA. Mouse peritoneal neutrophils were elicited by i.p. injection of thyioglycollate, with peritoneal lavage after 4 hours.

For NLRP3 activation in vitro, cells were primed with LPS (100 ng/ml) for 4 hours, then washed with RPMI. For some studies, cells were pretreated with inhibitors for 15–30 minutes prior to ATP or histone addition. Cells were treated with ATP or histones for 45–60 minutes. Cell-free supernatants were harvested and stored at −80°C until use.

Western blotting

Cell lysates were generated with RIPA buffer (Millipore, Billerica, MA) containing protease inhibitors (Roche). Total protein estimations were determined by BCA assay (Sigma). For lysates, 12 µg total protein was loaded per well for PAGE. Lysates or culture supernatants were separated by SDS-PAGE and blotted onto nitrocellulose membranes (Bio-Rad, Hercules, CA). Membranes were probed with anti-mouse IL-1β antibody (Cell Signaling Technology, Danvers, MA) followed by peroxidase-conjugated anti-rabbit IgG antibody (Jackson Immunoresearch), and visualized with chemiluminescent substrate (Denville Scientific, South Plainfield, NJ).

ELISA

Cytokine ELISAs were from R&D Systems, mouse albumin ELISAs were from Bethyl Laboratories (Montgomery, TX), and were performed per the manufacturer recommendations. Histone ELISAs were from Roche. Purified mixed calf thymus histones were used to generate standard curves as described (23).

Flow cytometry

Cells were analyzed on a BD LSR-II flow cytometer equipped with FACSDiva software (both from BD biosciences, San Jose, CA). Data was analyzed using FlowJo software (TreeStar, Ashland, OR). Greater than 2×10^4 cells with the forward and side scatter properties of mononuclear cells were analyzed from each sample. ROS production was determined by CellRox Deep Red oxidative stress reagent (5 µM; Life Technologies).

Confocal microscopy

The following antibodies were used for immunofluorescent labeling: anti-claudin-3 (Life Technologies), anti-rabbit IgG-FITC (Vector Laboratories, Burlingame, CA), anti-occludin-AlexaFluor[488] (Life Technologies), anti-histone H2A/H4 (BWA3), anti-mouse IgG-TRITC (Jackson Immunoresearch), anti-mouse Ly6G-AlexaFluor[647] (eBioscience, San Diego, CA), anti-mouse CD11c-AlexaFluor[488] (eBioscience), anti-mouse surfactant A (Millipore), anti-rabbit IgG-AlexaFluor[647] (Jackson Immunoresearch). Slides were mounted with ProLong Gold anti-fade reagent containing DAPI (Life Technologies). Digital monochromatic images were acquired on a Nikon A-1 confocal system with Nikon Elements software and pseudocolored. For quantitative analysis of histone-associated cells, greater than 200 histone-associated cells were analyzed per lung (n=3 mice) for cell type-specific labeling (neutrophil, macrophage, or type II alveolar epithelial cells). The percentage of histone-associated cells that were also labeled for the cell type-specific marker is displayed.

RT-PCR

RNA was harvested by the TRIzol (Sigma) method and treated with DNase to remove any contaminating genomic DNA. cDNA was generated (oligo dT primers) and RT-PCR (SYBR) was performed using reagents from Life Technologies on a 7500 real-time PCR System (Applied Biosystems, Foster City, CA). Results were analyzed by the 2^{-ddCt} method for relative quantitation and normalized to GAPDH. Primers (Life Technologies) used for amplification were as follows: GAPDH, 5′ CTTCAACAGCAACTCCCACTCTTCC 3′

(Fwd) and 5′ GGTGGTCCAGGGTTTCTTACTCC 3′ (Rev); IL-1β, 5′
CCTGCTGGTGTGTGACGTTC 3′ (Fwd) and 5′ CAGCACGAGGCTTTTTGTTGT 3′
(Rev).

Statistical analysis

Data were expressed as mean ± SEM. Data was analyzed using GraphPad Prism 6 graphing
and statistical analysis software (GraphPad Inc., La Jolla, CA). Significant differences
between sample means were determined using Mann-Whitney U or Kruskal-Wallis followed
by Dunn's Multiple Comparison Test as appropriate. A p value <0.05 was considered to be
significant.

RESULTS

The NLRP3 inflammasome is essential for the development of experimental ALI

In the LPS-induced model of ALI, the absence of NLRP3 or caspase-1 reduced the albumin
leak by 61% and 73%, respectively (Fig. 1A). IL-1β levels in BALF were reduced by 79%
and 78% in NLRP3$^{-/-}$ and caspase-1$^{-/-}$ mice, respectively, compared to wild type mice
(Fig. 1B). However, a NLRP3 inflammasome-independent cytokine, TNF, was not affected
by the absence of NLRP3 or caspase-1 (Fig. 1C). NLRP3$^{-/-}$ or caspase-1$^{-/-}$ mice also had
reduced numbers of neutrophils found in BALF during LPS-induced ALI, although
caspase-1$^{-/-}$ mice did not reach statistical significance (Fig. 1D).

Figure 1E shows the histologic features (using H&E staining and confocal
immunofluorescent microscopy) of wild type sham lungs in which alveolar and interstitial
spaces were free of inflammatory cells. In wild type ALI lungs, neutrophils were present in
alveolar walls and in interstitial spaces. In caspase 1$^{-/-}$ or NLRP3$^{-/-}$ mice, neutrophils were
present but their numbers were attenuated, in agreement with the data in Fig. 1D.

In Figure 1E, the tight junction proteins (claudin-3 and occludin) showed a strong linear
pattern staining in sham lung (arrows). ALI induced in wild type mice a dramatic reduction
in immunostaining in alveolar walls for the two tight junction proteins. In either caspase 1$^{-/-}$
or NLRP3$^{-/-}$ mice, the intensity of the immunostaining was protected, compared to wild
type ALI, but there were scattered areas in alveolar walls in which there were discontinuities
in the alveolar walls (arrowheads). These findings are in agreement with reduced alveolar
albumin leak in NLRP3$^{-/-}$ and caspase-1$^{-/-}$ mice (Fig. 1A), and are consistent with the
observation that both caspase-1 and NLRP3 are required for the full development of ALI.

Both macrophages and neutrophils are required for IL-1β production during ALI

IL-1β was detected in BALF in a time-dependent manner during LPS-induced ALI (Fig.
2A). Depletion of alveolar macrophages by administration of clodronate liposomes reduced
the levels of IL-1β detected in BALF by 70% (Fig. 2B). In addition, levels of IL-1β found in
BALF during ALI were reduced 54% by neutrophil depletion (Fig. 2C). This observation
was surprising, given that neutrophils produced only a fraction of the IL-1β that
macrophages produced when the NLRP3 inflammasome was activated in vitro (Fig. 2D).

These findings suggested that a neutrophil-derived product may be activating the NLRP3 inflammasome during ALI in vivo.

Neutrophils are the source of extracellular histones during ALI

Extracellular histones are known to be released by neutrophils in the form of neutrophil extracellular traps (NETs) (28). Extracellular histones have recently been reported to act as activators of the NLRP3 inflammasome (29, 30). We have previously reported that extracellular histones are important drivers of C5a-induced ALI (23). Tissue sections of LPS-induced ALI lung revealed diffuse presence of histones in lung after 6 hours (Fig. 3A). The antibody used (clone BWA3) does not bind to histones present in intact nucleosomes (26). Extracellular histones appeared in BALF in a time-dependent manner during LPS-induced ALI (Fig. 3B). The depletion of neutrophils significantly reduced the levels of extracellular histones in BALF (Fig. 3C). Confocal microscopic analysis of ALI lung revealed that histones were primarily associated with neutrophils (Fig. 3D, arrows). Histone labeling was localized in the nuclear and perinuclear space, which may suggest chromatin breakdown and histone release from genomic DNA, as described for NET formation (Fig. 3D) (28, 31). A small proportion of histone-associated cells were cell types other than neutrophils (Fig. 3D, arrowhead). A quantitative analysis revealed that >90% of histone-associated cells were neutrophils, and about 4% were CD11c^{+} macrophages/dendritic cells (Fig. 3E). Together, these results suggest that during ALI, extracellular histones were released from neutrophils.

Release of histones by neutrophils in response to C5a

We have previously reported that extracellular histone presence during ALI was dependent on the C5a receptors C5aR and C5L2 (23). Whether C5a acts directly on neutrophils to induced histone release is not known. We incubated purified bone marrow neutrophils with LPS, C5a, or PMA (a known inducer of NETs (31)). Confocal microscopic images revealed that C5a and PMA led to histone release (Fig. 4A and 4B), but LPS did not (data not shown). Histones were present in the nuclear and perinuclear space, in agreement with our findings in vivo (Fig. 4B and Fig. 3D). Quantitation of histones in culture supernatants of likewise treated neutrophils revealed significantly increased levels of histones in PMA or C5a-treated conditions, compared to untreated cells or LPS-treated cells (Fig. 4C). Together, these results demonstrate direct effects of C5a on neutrophils that lead to extracellular histone release, and suggests that complement activation during ALI is requisite for optimal histone release, in agreement with our previous findings (23).

Extracellular histones activate the NLRP3 inflammasome

We hypothesized that extracellular histones were acting as NLRP3 inflammasome activators during ALI. Administration (i.t.) of exogenous histones (250 μg) resulted in intense ALI compared to sham (PBS) or instillation of BSA i.t. (250 μg) (Fig. 5A), and levels of IL-1β were significantly elevated compared to levels in control (sham or BSA) BALFs (Fig. 5B). Antibody-mediated neutralization of extracellular histones (H2A and H4) reduced the levels of IL-1β in BALF during LPS-induced ALI by 35%, compared to an isotype control antibody (Fig. 5C). However, in vitro treatment of macrophages with histones did not induce

the transcription of IL-1β mRNA (Fig. 5D), suggesting a role for extracellular histones during NLRP3 activation, but not in NLRP3 priming.

Macrophages were primed with LPS then treated with histones. ATP, a known activator of the NLRP3 inflammasome, was used as a positive control. Results showed that histones (Hist) induced a very low level of IL-1β release in the absence of LPS pretreatment (Fig. 5E, bars on left side). However, in LPS-primed macrophages, histones induced robust IL-1β release in a dose-dependent manner (EC_{50} = 65 μg/ml, Fig. 5E), in agreement with recent reports using Kupffer cells and dendritic cells (29, 30). Similar experiments performed with mouse neutrophils showed comparable results (EC_{50} = 40 μg/ml, Fig. 5F). Western blots for IL-1β were performed to assess the processing of pro-IL-1β (31 kDa) into the biologically active form (17 kDa). Indeed, macrophages pretreated with LPS and then exposed to histones released processed (mature) IL-1β into the culture supernatant fluids (Fig. 5G). To control for contaminating DNA or RNA, which might be present in histone preparations, histones were pretreated with DNase or RNase prior to the administration of histones to macrophages. This procedure appeared to rule out results due to contaminating DNA or RNA on inflammasome activation (Fig. 5H). Instead, the inflammasome activation induced by histones was due to the protein fraction of the histone preparations (proteinase K-treated, Fig. 5H). Together, these results demonstrate that histones directly activated the inflammasome in both LPS-primed macrophages and neutrophils, and during LPS-induced ALI.

Mechanism of macrophage NLRP3 inflammasome activation by extracellular histones

We next investigated the molecular mechanisms for inflammasome activation by extracellular histones. Macrophages from wild type or NLRP3$^{-/-}$ mice were primed with LPS, followed by ATP or histones (1 mM and 50 μg/ml, respectively). LPS pretreatment followed by the addition of ATP or histones showed much amplified release of IL-1β from wild type cells but not from NLRP3$^{-/-}$ cells, indicating that indeed histones activated the NLRP3 inflammasome in macrophages (Fig. 6A). Lysates from LPS primed wild type and NLRP3$^{-/-}$ macrophages contained similar levels of pro-IL-1β, suggesting that the defect in IL-1β release in NLRP3$^{-/-}$ cells was not in the LPS priming, but involved inflammasome activation (data not shown). A critical driver of NLRP3 activation involves the development of membrane ionic permeability and resulting ionic imbalance (4, 9, 32–34). Macrophages exposed to histones (50 μg/ml) displayed an ionic imbalance, evidenced by significant cell swelling as measured by forward scatter in flow cytometry (Fig. 6B). Macrophage swelling in the presence of histones was time-dependent (Fig. 6C). Movement of K^+ from the intracellular to the extracellular space is a known requirement for NLRP3 inflammasome activation (4). The exogenous elevation of extracellular K^+ (to inhibit K^+ efflux) sharply reduced the amount of IL-1β released following stimulation with LPS and ATP or histones (Fig. 6D). When cells were treated with the intracellular Ca^{+2} chelator, BAPTA, it ablated IL-1β release in response to ATP and substantially reduced histone-induced release of IL-1β (Fig. 6E). The IL-1β that was released by histones in the presence of BAPTA was fully processed (17 kDa, data not shown). Treatment with an inositol triphosphate receptor (InsP3R) inhibitor, 2-APB, which prevents Ca^{+2} release from intracellular stores, resulted in complete suppression of IL-1β release in response to ATP, but only partial inhibition of

histone-induced IL-1β release (Fig. 6F). Therefore, Ca^{+2} release from intracellular stores appeared to be partially responsible for histone-induced NLRP3 inflammasome activation. Treatment of macrophages with histones induced ROS production (Fig. 6G), and treatment with a ROS scavenger (NAC) significantly reduced IL-1β release in response to histones (Fig. 6H). Therefore, histone-induced NLRP3 activation appeared to be at least partially dependent on the generation of ROS. LPS pretreated wild type macrophages, but not caspase-1$^{-/-}$ macrophages, produced high levels of IL-1β in response to either ATP or histones (Fig. 6I). Analysis of cell lysates indicated that caspase-1$^{-/-}$ cells contained similar amounts of pro-IL-1β as wild type cells, indicating that the defect in IL-1β release was during inflammasome activation and not related to LPS priming (data not shown). Caspase-1$^{-/-}$ mice are known to also be deficient in caspase-11 (35), due to a naturally occurring dysfunctional allele in the 129 background. Therefore, we used a caspase-1-specific inhibitor (Y-VAD-CMK) to selectively block caspase-1. Results showed that specific inhibition of caspase-1 resulted in significantly reduced levels of IL-1β in response to LPS and ATP or histones, compared to vehicle-treated macrophages (Fig. 6J). Phagocytosis was not required for histone-induced NLRP3 inflammasome activation, in contrast to particulate (e.g., silica) NLRP3 inflammasome activators (Fig. 6K) (36). Taken together, these results demonstrated that histone-induced IL-1β release by macrophages was dependent on NLRP3, caspase-1, and K^+ efflux, and partially dependent on elevated $[Ca^{+2}]i$ and ROS generation. These requirements for histone-induced NLRP3 inflammasome activation are in agreement with other known NLRP3 activators (4).

Influence of individual histones on inflammasome activation

There are four core histone proteins (H2A, H2B, H3, and H4) and one linker histone (H1). We tested whether these individual histones had different inflammasome-activating properties. LPS-pretreated macrophages were treated with mixed calf thymus histones or individual recombinant or purified histones. Results showed that histone H1 had the highest level of inflammasome-activating ability (Fig. 7A). In addition, IL-1β release was highly correlated with the amount of cell swelling induced by individual histone monomers (Fig. 7B). Therefore, there are significant differences in inflammasome-activating abilities between the individual histones.

Full extracellular histone release during ALI requires the NLRP3 inflammasome

We have demonstrated that extracellular histones activated the NLRP3 inflammasome during ALI. However, whether the NLRP3 inflammasome itself contributes to histone release is not known. We measured histone levels in BALF from wild type, NLRP3$^{-/-}$, and caspase-1$^{-/-}$ mice during LPS-induced ALI. Results showed that full extracellular histone presence was dependent on NLRP3 (Fig. 8A) and caspase-1 (Fig. 8B), although NLRP3$^{-/-}$ mice did not reach statistical significance. These results suggest that a positive feedback mechanism may exist between extracellular histones and NLRP3 inflammasome activation (likely resulting in IL-1β-dependent neutrophil recruitment) that propagates and exacerbates ALI.

Evidence for the histone/inflammasome inflammatory mechanism in other ALI models

To determine whether extracellular histones and the inflammasome (IL-1β production) have a role in other models of ALI, we measured these mediators in BALF from C5a-induced and IgG immune complex-induced ALI. As previously described, i.t. instillation of C5a (500 ng) resulted in robust ALI (defined by albumin leak, Fig 9A, left panel) (23). Both histone and IL-1β levels in BALF were significantly elevated in this model (Fig. 9A, middle and right panel, respectively). Distal airway deposition of IgG immune complexes also resulted in ALI, as previously described (Fig. 9B, left panel) (27). Again, both histone and IL-1β levels were elevated in this model (Fig. 9B, middle and right panel, respectively). Collectively, these data suggest that interactions between extracellular histones and the NLRP3 inflammasome may be a common inflammatory mechanism during ALI, and may extend to other inflammatory conditions in the lung.

DISCUSSION

In this report, we have demonstrated that full development of ALI requires the engagement of the NLRP3 inflammasome. Extracellular histones were identified as activators of the NLRP3 inflammasome, in agreement with two recent reports (29, 30). Macrophages exposed to histones processed and released mature IL-1β. During ALI, the appearance of extracellular histones and IL-1β in BALF was dependent on both neutrophils and macrophages, suggesting a synergistic interaction between the two cell types. On the basis of immunostaining and cell depletion studies, neutrophils were identified as the primary source of histones during ALI, and neutrophils released histones in response to C5a treatment in vitro. Finally, the NLRP3 inflammasome was required for full extracellular histone presence during development of ALI, likely due to the role of IL-1β in promoting neutrophil recruitment (thus neutrophil-dependent histone release). Taken together, these results identify a novel inflammatory mechanism involving extracellular histones and the NLRP3 inflammasome during development of ALI (Fig. 10).

The mechanism of cell "sensing" of extracellular histones remains unknown. It is not clear whether histones bind specific surface receptors or interact non-specifically with plasma membranes. NLRP3 inflammasome activation involves the movement of ions (K^+ extrusion) which suggests that histone-induced plasma membrane permeability may be the critical activation step. Histones have been reported to increase conductance non-specifically (i.e., not bound to a specific receptor) in purified lipid bilayers by forming a channel (37). Importantly, histones can interact with phospholipids (38), and may insert directly into the cell membrane by binding the negatively charged phosphate groups, much like they bind the phosphodiester bonds of DNA. There are several pore-forming toxins produced by bacteria that can cause membrane depolarization and osmotic imbalance leading to activation of the NLRP3 inflammasome (39, 40). A similar mechanism of NLRP3 inflammasome activation has been described for sublytic levels of the complement membrane attack complex (41). Histones may activate the NLRP3 inflammasome in a similar manner as these membrane pore-forming proteins.

ALI/ARDS remains a significant clinical problem with no current FDA-approved drug. Due to the reality that ALI/ARDS patients entering the intensive care unit have often already

developed clinical disease, therapeutics targeting not only the initiation but the ongoing propagation of ALI/ARDS are likely necessary. Here we have described one potential mechanism of inflammatory propagation during experimental ALI that involves extracellular histones which activate the NLRP3 inflammasome. Certainly, either mediator/pathway by itself is pro-inflammatory. However, we show that extracellular histones are produced during ALI and activate the NLRP3 inflammasome, promoting the recruitment of neutrophils (and additional appearance of histones in the extracellular space), suggesting positive feedback and a potential mechanism of inflammatory propagation (Fig. 10). Therefore, therapeutic targeting of extracellular histones or IL-1β may be an attractive option for combating ALI/ARDS and other inflammatory diseases.

Acknowledgments

ABBREVIATIONS

2-APB	2-aminoethyl diphenylborinate
ALI	acute lung injury
ARDS	acute respiratory distress syndrome
BALF	bronchoalveolar lavage fluids
CAPS	cryopyrin-associated periodic syndrome
IL-1RA	IL-1 receptor antagonist
NAC	N-acetyl-L-cysteine
NOMID	neonatal-onset multisystem inflammatory disease
ROS	reactive oxygen species

References

1. Goss CH, Brower RG, Hudson LD, Rubenfeld GD. Incidence of acute lung injury in the United States. Crit Care Med. 2003; 31:1607–1611. [PubMed: 12794394]

2. Angus DC, Linde-Zwirble WT, Lidicker J, Clermont G, Carcillo J, Pinsky MR. Epidemiology of severe sepsis in the United States: analysis of incidence, outcome, and associated costs of care. Crit Care Med. 2001; 29:1303–1310. [PubMed: 11445675]

3. Matthay MA, Ware LB, Zimmerman GA. The acute respiratory distress syndrome. J Clin Invest. 2012; 122:2731–2740. [PubMed: 22850883]

4. Franchi L, Munoz-Planillo R, Nunez G. Sensing and reacting to microbes through the inflammasomes. Nat Immunol. 2012; 13:325–332. [PubMed: 22430785]

5. Bauernfeind FG, Horvath G, Stutz A, Alnemri ES, MacDonald K, Speert D, Fernandes-Alnemri T, Wu J, Monks BG, Fitzgerald KA, Hornung V, Latz E. Cutting edge: NF-kappaB activating pattern recognition and cytokine receptors license NLRP3 inflammasome activation by regulating NLRP3 expression. J Immunol. 2009; 183:787–791. [PubMed: 19570822]

6. Bauernfeind F, Bartok E, Rieger A, Franchi L, Nunez G, Hornung V. Cutting edge: reactive oxygen species inhibitors block priming, but not activation, of the NLRP3 inflammasome. J Immunol. 2011; 187:613–617. [PubMed: 21677136]

7. Dostert C, Guarda G, Romero JF, Menu P, Gross O, Tardivel A, Suva ML, Stehle JC, Kopf M, Stamenkovic I, Corradin G, Tschopp J. Malarial hemozoin is a Nalp3 inflammasome activating danger signal. PLoS One. 2009; 4:e6510. [PubMed: 19652710]

8. Masters SL, Dunne A, Subramanian SL, Hull RL, Tannahill GM, Sharp FA, Becker C, Franchi L, Yoshihara E, Chen Z, Mullooly N, Mielke LA, Harris J, Coll RC, Mills KH, Mok KH, Newsholme P, Nunez G, Yodoi J, Kahn SE, Lavelle EC, O'Neill LA. Activation of the NLRP3 inflammasome by islet amyloid polypeptide provides a mechanism for enhanced IL-1β in type 2 diabetes. Nat Immunol. 2010; 11:897–904. [PubMed: 20835230]

9. Lee GS, Subramanian N, Kim AI, Aksentijevich I, Goldbach-Mansky R, Sacks DB, Germain RN, Kastner DL, Chae JJ. The calcium-sensing receptor regulates the NLRP3 inflammasome through Ca2+ and cAMP. Nature. 2012; 492:123–127. [PubMed: 23143333]

10. Dolinay T, Kim YS, Howrylak J, Hunninghake GM, An CH, Fredenburgh L, Massaro AF, Rogers A, Gazourian L, Nakahira K, Haspel JA, Landazury R, Eppanapally S, Christie JD, Meyer NJ, Ware LB, Christiani DC, Ryter SW, Baron RM, Choi AM. Inflammasome-regulated cytokines are critical mediators of acute lung injury. Am J Respir Crit Care Med. 2012; 185:1225–1234. [PubMed: 22461369]

11. Makabe H, Kojika M, Takahashi G, Matsumoto N, Shibata S, Suzuki Y, Inoue Y, Endo S. Interleukin-18 levels reflect the long-term prognosis of acute lung injury and acute respiratory distress syndrome. J Anesth. 2012; 26:658–663. [PubMed: 22639237]

12. Jordan JA, Guo RF, Yun EC, Sarma V, Warner RL, Crouch LD, Senaldi G, Ulich TR, Ward PA. Role of IL-18 in acute lung inflammation. J Immunol. 2001; 167:7060–7068. [PubMed: 11739527]

13. Kuipers MT, Aslami H, Janczy JR, van er Sluijs KF, Vlaar AP, Wothuis EK, Choi G, Roelofs JJ, Flavell RA, Sutterwala FS, Bresser P, Leemans JC, van der Poll T, Schultz MJ, Wieland CW. Ventilator-induced lung injury is mediated by the NLRP3 inflammasome. Anesthesiology. 2012; 116:1104–1115. [PubMed: 22531249]

14. Wu J, Yan Z, Schwartz DE, Yu J, Malik AB, Hu G. Activation of NLRP3 inflammasome in alveolar macrophages contributes to mechanical stretch-induced lung inflammation and injury. J Immunol. 2013; 190:3590–3599. [PubMed: 23436933]

15. Mulligan MS, Ward PA. Immune complex-induced lung and dermal vascular injury. Differing requirements for tumor necrosis factor-alpha and IL-1. J Immunol. 1992; 149:331–339. [PubMed: 1318904]

16. Gasse P, Mary C, Guenon I, Noulin N, Charron S, Schnyder-Candrian S, Schnyder B, Akira S, Quesniaux VF, Lagente V, Ryffel B, Couillin I. IL-1R1/MyD88 signaling and the inflammasome are essential in pulmonary inflammation and fibrosis in mice. J Clin Invest. 2007; 117:3786–3799. [PubMed: 17992263]

17. Xiang M, Shi X, Li Y, Xu J, Yin L, Xiao G, Scott MJ, Billiar TR, Wilson MA, Fan J. Hemorrhagic shock activation of NLRP3 inflammasome in lung endothelial cells. J Immunol. 2011; 187:4809–4817. [PubMed: 21940680]

18. dos Santos G, Kutuzov MA, Ridge KM. The inflammasome in lung diseases. Am J Physiol Lung Cell Mol Physiol. 2012; 303:L627–633. [PubMed: 22904168]

19. Abrams ST, Zhang N, Manson J, Liu T, Dart C, Baluwa F, Wang SS, Brohi K, Kipar A, Yu W, Wang G, Toh CH. Circulating histones are mediators of trauma-associated lung injury. Am J Crit Care Med. 2013; 187:160–169.

20. Xu J, Zhang X, Pelayo R, Monestier M, Ammollo CT, Semeraro F, Taylor FB, Esmon NL, Lupu F, Esmon CT. Extracellular histones are major mediators of death in sepsis. Nat Med. 2009; 15:1318–1321. [PubMed: 19855397]

21. Allam R, Scherbaum CR, Darisipudi MN, Mulay SR, Hagele H, Lichtnekert J, Hagemann JH, Rupanagudi KV, Ryu M, Schwarzenberger C, Hohenstein B, Hugo C, Uhl B, Reichel CA, Krombach F, Monestier M, Liapis H, Moreth K, Schaefer L, Anders HJ. Histones from dying renal cells aggravate kidney injury via TLR2 and TLR4. J Am Soc Nephrol. 2012; 23:1375–1388. [PubMed: 22677551]

22. Huang H, Evankovich J, Yan W, Nace G, Zhang L, Ross M, Liao X, Billiar T, Xu J, Esmon CT, Tsung A. Endogenous histones function as alarmins in sterile inflammatory liver injury through Toll-like receptor 9 in mice. Hepatology. 2011; 54:999–1008. [PubMed: 21721026]

23. Bosmann M, Grailer JJ, Russkamp NF, Ruemmler R, Monestier M, Zetoune FS, Sarma JV, Ward PA. Extracellular histones are essential effectors of C5aR and C5L2-dependent tissue damage and inflammation in acute lung injury. FASEB J. 2013; 27:5010–5021. [PubMed: 23982144]

24. Kovarova M, Hesker PR, Jania L, Nguyen M, Snouwaert JN, Xiang Z, Lommatzsch SE, Huang MT, Ting JP, Koller BH. NLRP1-dependent pyroptosis leads to acute lung injury and morbidity in mice. J Immunol. 2012; 189:2006–2016. [PubMed: 22753929]

25. Kuida K, Lippke JA, Ku G, Harding MW, Livingston DJ, Su MS, Flavell RA. Altered cytokine export and apoptosis in mice deficient in interleukin-1 beta converting enzyme. Science. 1995; 267:2000–2003. [PubMed: 7535475]

26. Monestier M, Fasy TM, Losman MJ, Novick KE, Muller S. Structure and binding properties of monoclonal antibodies to core histones from autoimmune mice. Mol Immunol. 1993; 30:1069–1075. [PubMed: 8366857]

27. Bosmann M, Grailer JJ, Zhu K, Matthay MA, Sarma JV, Zetoune FS, Ward PA. Anti-inflammatory effects of β2 adrenergic receptor agonists in experimental acute lung injury. FASEB J. 2012; 26:2137–2144. [PubMed: 22318967]

28. Saffarzadeh M, Juenemann C, Queisser MA, Lochnit G, Barreto G, Galuska SP, Lohmeyer J, Preissner KT. Neutrophil extracellular traps directly induce epithelial and endothelial cell death: a predominant role of histones. PLoS One. 2012; 7:e32366. [PubMed: 22389696]

29. Allam R, Darisipudi MN, Tschopp J, Anders HJ. Histones trigger sterile inflammation by activating the NLRP3 inflammasome. Eur J Immunol. 2013 Epub ahead of print. 10.1002/eji.201243224

30. Huang H, Chen HW, Evankovich J, Yan W, Rosborough BR, Nace GW, Ding Q, Loughran P, Beer-Stolz D, Billiar TR, Esmon CT, Tsung A. Histones activate the NLRP3 inflammasome in Kupffer cells during sterile inflammatory liver injury. J Immunol. 2013; 191:2665–2679. [PubMed: 23904166]

31. Brinkman V, Reichard U, Goosmann C, Fauler B, Uhlemann Y, Weiss DS, Weinrauch Y, Zychlinsky A. Neutrophil extracellular traps kill bacteria. Science. 2004; 303:1532–1535. [PubMed: 15001782]

32. Murakami T, Ockinger J, Yu J, Byles V, McColl A, Hofer AM, Horng T. Critical role for calcium mobilization in activation of the NLRP3 inflammasome. Proc Natl Acad Sci USA. 2012; 109:11282–11287. [PubMed: 22733741]

33. Andrei C, Margiocco P, Poggi A, Lotti LV, Torris MR, Rubartelli A. Phospholipases C and A2 control lysosome-mediated IL-1beta secretion: Implications for inflammatory processes. Proc Natl Acad Sci USA. 2004; 101:9745–9750. [PubMed: 15192144]

34. Dostert C, Petrilli V, Van Bruggen R, Steele C, Mossman BT, Tschopp J. Innate immune activation through the Nalp3 inflammasome sensing of asbestos and silica. Science. 2008; 320:674–677. [PubMed: 18403674]

35. Kayagaki N, Warming S, Lamkanfi M, Vande Walle L, Louie S, Dong J, Newton K, Qu Y, Liu J, Heldens S, Zhang J, Lee WP, Roose-Girma M, Dixit VM. Non-canonical inflammasome activation targets caspase-11. Nature. 2011; 479:117–121. [PubMed: 22002608]

36. Franchi L, Eigenbrod T, Munoz-Planillo R, Nunez G. The inflammasome: a caspase-1-activation platform that regulates immune responses and disease pathogenesis. Nat Immunol. 2009; 10:241–147. [PubMed: 19221555]

37. Kleine TJ, Lewis PN, Lewis SA. Histone-induced damage of a mammalian epithelium: the role of protein and membrane structure. Am J Physiol. 1997; 273:C1925–1936. [PubMed: 9435498]

38. Pereira LF, Marco FM, Boimorto R, Caturla A, Bustos A, De la Concha EG, Subiza JL. Histones interact with anionic phospholipids with high avidity; is relevance for the binding of histone-antihistone immune complexes. Clin Exp Immunol. 1994; 97:175–180. [PubMed: 8050163]

39. Harder J, Franchi L, Munoz-Planillo R, Park JH, Reimer T, Nunez G. Activation of the Nlrp3 inflammasome by Streptococcus pyogenes requires streptolysin O and NF-kappa B activation but

proceeds independently of TLR signaling and P2X7 receptor. J Immunol. 2009; 183:5823–5829. [PubMed: 19812205]

40. Munoz-Planillo R, Franchi L, Miller LS, Nunez G. A critical role for hemolysins and bacterial lipoproteins in Staphylococcus aureus-induced activation of the Nlrp3 inflammasome. J Immunol. 2009; 183:3942–3948. [PubMed: 19717510]

41. Triantafilou K, Hughes TR, Triantafilou M, Morgan BP. The complement membrane attack complex triggers intracellular Ca2+ fluxes leading to NLRP3 inflammasome activation. J Cell Sci. 2013; 126:2903–2913. [PubMed: 23613465]
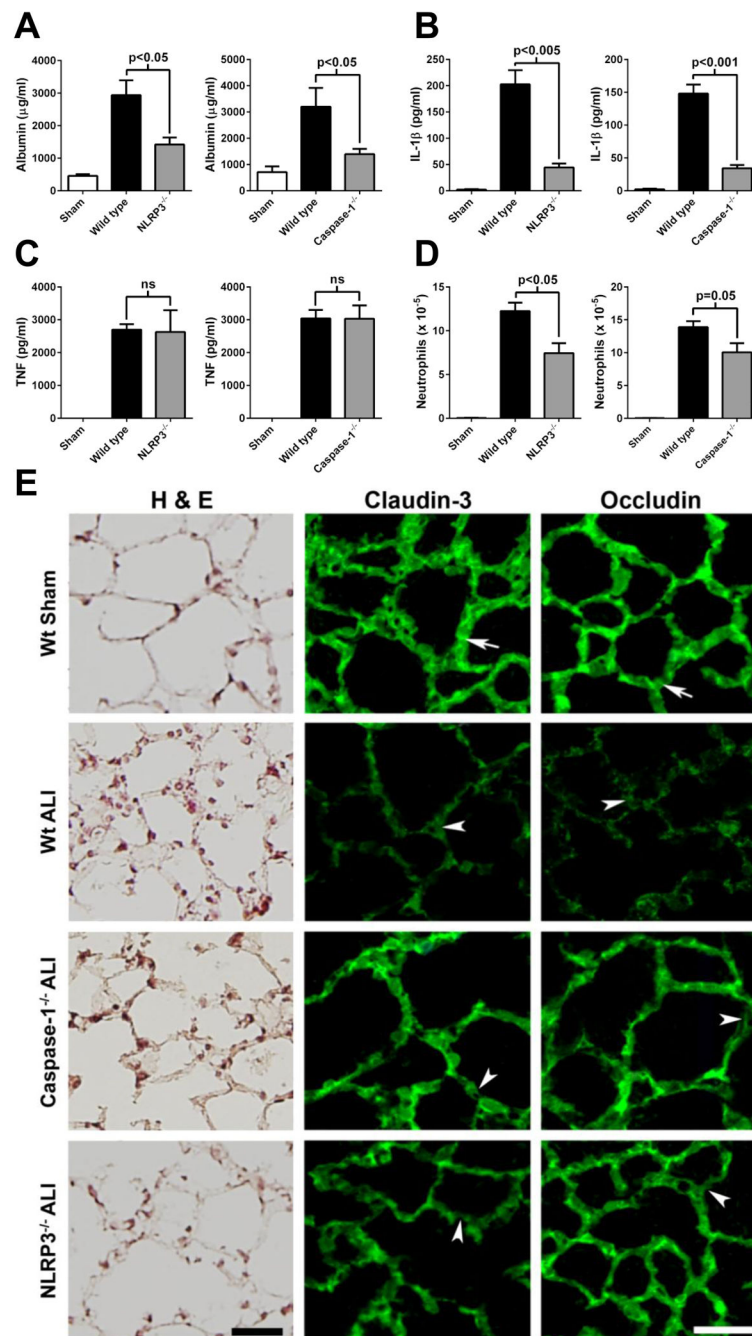
Figure 1.
The NLRP3 inflammasome and caspase-1 mediate LPS-induced ALI. Wild type or the indicated knockout mice received 60 µg LPS (i.t.) under anesthesia. Sham mice received sterile saline. BALFs were harvested 8 hours later and levels of A) albumin, B) IL-1β, and C) TNF were determined by ELISA. D) Neutrophil numbers in BALFs were counted (n   5 mice per group). E) Lung epithelial barrier integrity in ALI. Tight junctional (Tj) proteins claudin-3 and occludin immunostaining in lung of mice subjected to LPS-induced ALI (Wt ALI) showed defragmented and low intensity staining in alveolar septa (arrowhead)

indicating the loss of Tj between epithelial cells, compared with control (Wt sham) where both claudin-3 and occludin had a linear staining pattern (arrows). ALI in caspase-1$^{-/-}$ and NLRP3$^{-/-}$ mice induced only partial changes in linear staining of claudin-3 and occludin, indicating only limited alteration of Tj and lung epithelial barrier. Scale bar is 50 μm. Left hand side, H & E features of wild type sham lung, wild type ALI, and ALI in caspase-1$^{-/-}$ or NLRP3$^{-/-}$ mice. See text for details.

A

B

C

D
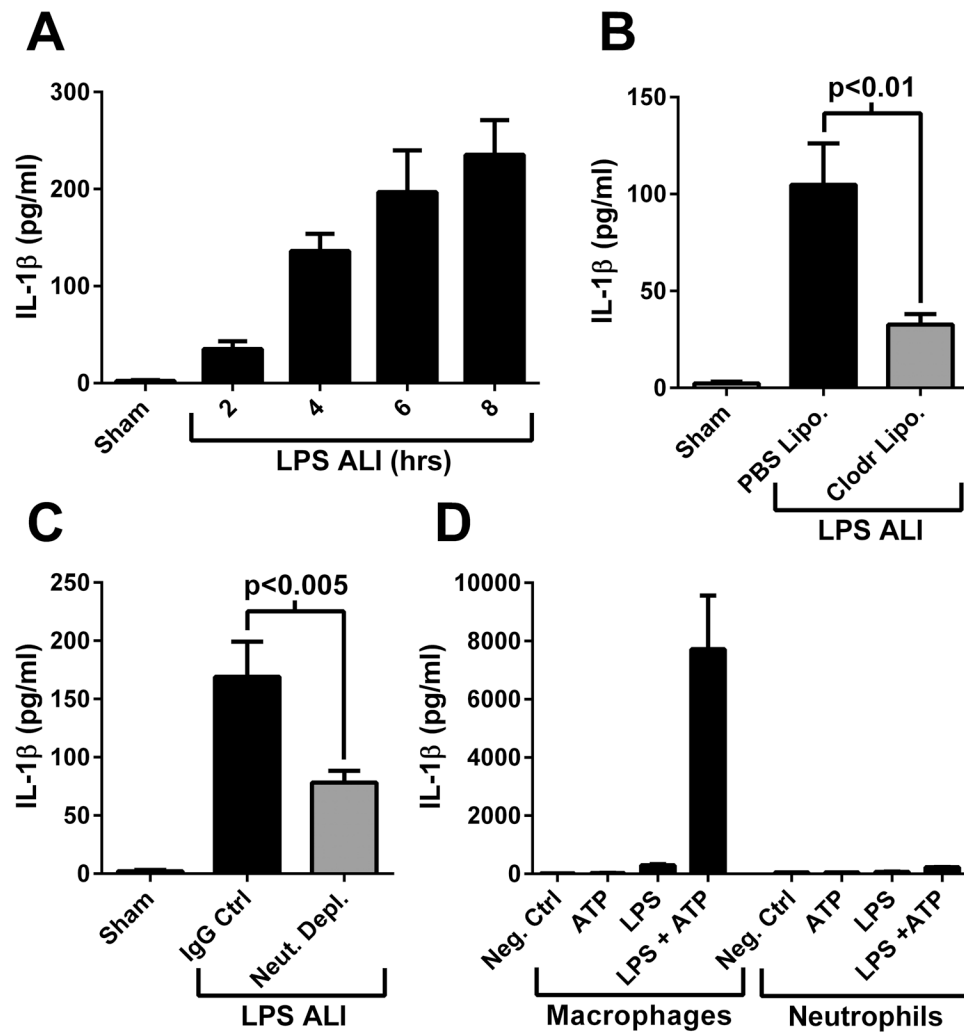
Figure 2.
IL-1β production is dependent on the presence of macrophages and neutrophils during ALI. A) IL-1β levels measured in BALF at time points during LPS-induced ALI (n 5 mice per group). B) IL-1β presence in BALF during ALI (8 hours) in control (PBS Lipo.) or macrophage depleted (Clodr Lipo.) mice (n 5 mice per group). C) IL-1β presence in BALF during ALI (8 hours) in control or neutrophil depleted mice (n 6 mice per group). D) IL-1β levels in culture supernatants from mouse peritoneal macrophages (left side) or neutrophils (right side) treated in the presence or absence of LPS (100 ng/ml) for 4 hrs followed by ATP (1 mM) for 45 min. Results are triplicate samples representative of 3 independent experiments.
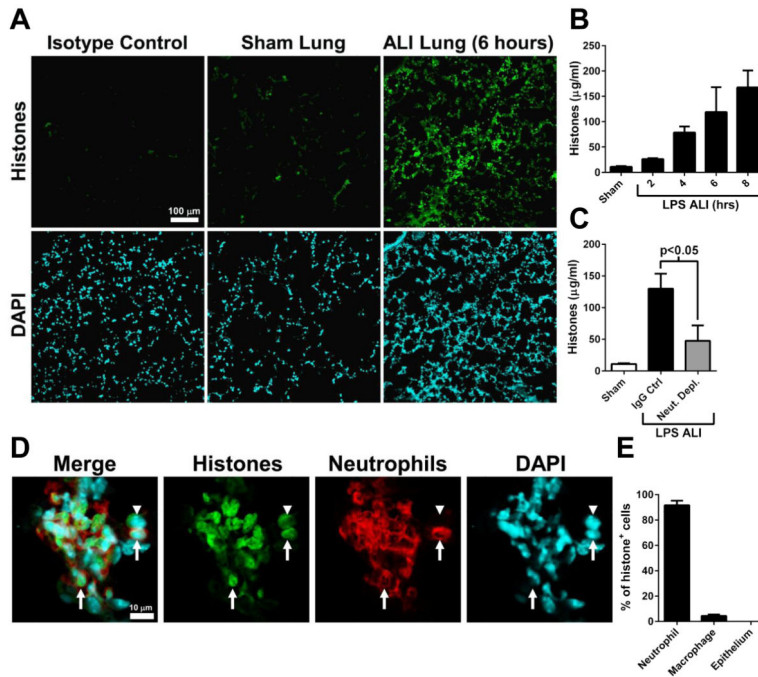
Figure 3.
Neutrophils are the source of extracellular histones during LPS-induced ALI. A) Histone detection (BWA3 antibody) in tissue sections from sham or ALI lung. The scale bar in A is for all images. B) Histones measured in BALF at time points during LPS-induced ALI (n 5 mice per group). C) Histone presence in BALF during ALI (8 hours) in control or neutrophil depleted mice (n 6 mice per group). D) ALI (6 hours) lung tissue sections were labeled for histones (BWA3 antibody) as well as neutrophils (Ly6G). Most histone-associated cells were neutrophils (arrows), however a small number of histone-associated cells were not neutrophils (arrowheads). The scale bar in D is for all images. E) Quantitative analysis of histone-associated cell subytpes. Tissues sections were labeled for histones as well as neutrophils (Ly6G), alveolar macrophages/dendritic cells (CD11c), or type II epithelial cells (surfactant A). The percentage of histone-associated cells that co-labeled with the cell type specific marker is shown (n=3 mice).
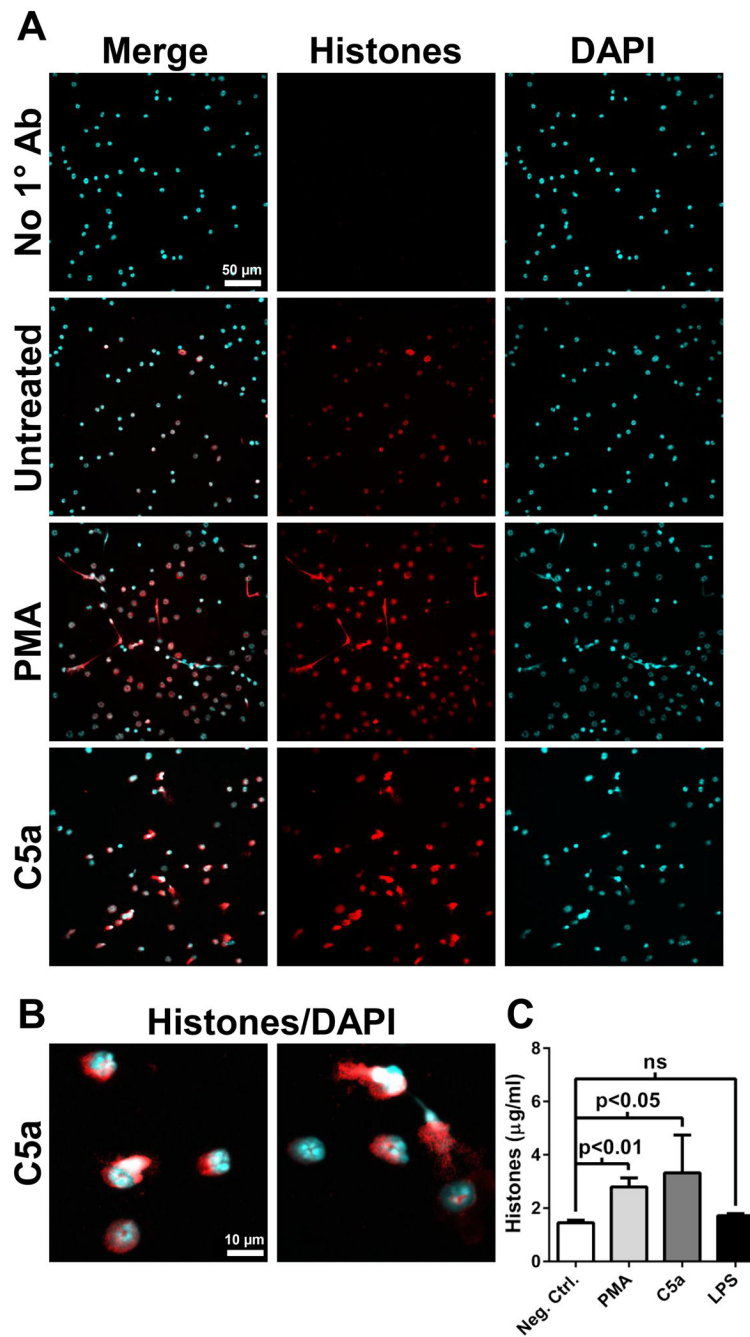
Figure 4.
Release of histones by neutrophils in vitro. A) Purified bone marrow neutrophils were incubated in the presence of PMA (50 ng/ml), C5a (1 μg/ml), or vehicle (untreated) for 90 min. Cells were fixed and histones were labeled with BWA3 antibody (H2A/H4). Images are representative of 2 independent experiments. The scale bar in A is for all images. B) Higher magnification images of C5a-treated neutrophils as described in A. The scale bar in B is for both images. C) Quantitation of histones present in culture supernatants of neutrophils treated as described in A (n=4 samples).
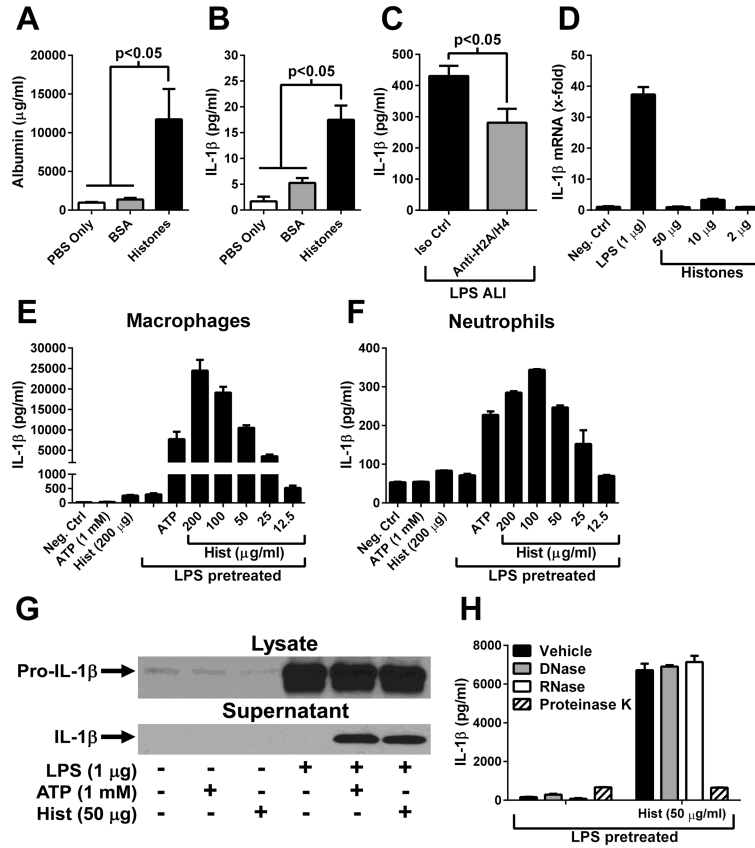
Figure 5.
Extracellular histones activate the inflammasome. A–B) Albumin and IL-1β levels in BALF 6 hours following i.t. administration of histones or BSA (250 μg). Sham animals received sterile PBS (n   5 mice per group). C) LPS-induced ALI in the presence of histone H2A/H4 neutralizing antibody (Anti-H2A/H4) or isotype control antibody. IL-1β levels found in BALF after 8 hours is shown (n=6–7 per group). D) RT-PCR analysis of IL-1β mRNA from mouse peritoneal macrophages treated in vitro for 3 hours with LPS or histones. E–F) Macrophages or neutrophils (5×10^5 each) were primed with LPS (100 ng/ml) for 4 hours, then treated with ATP or various concentrations of histones (Hist) for 45 min. The level of IL-1β in culture supernatants was determined by ELISA. G) Macrophages were treated as described in E. Cell lysates or culture supernatants were analyzed by Western blot for the presence of IL-1β. H) Macrophages were treated as in E, but histone preparations were pretreated with DNAse (10 U/ml), RNAse (10 U/ml) or proteinase K (20 U/ml) prior to cell treatment. In vitro experiments are triplicate samples representative of   3 independent experiments.
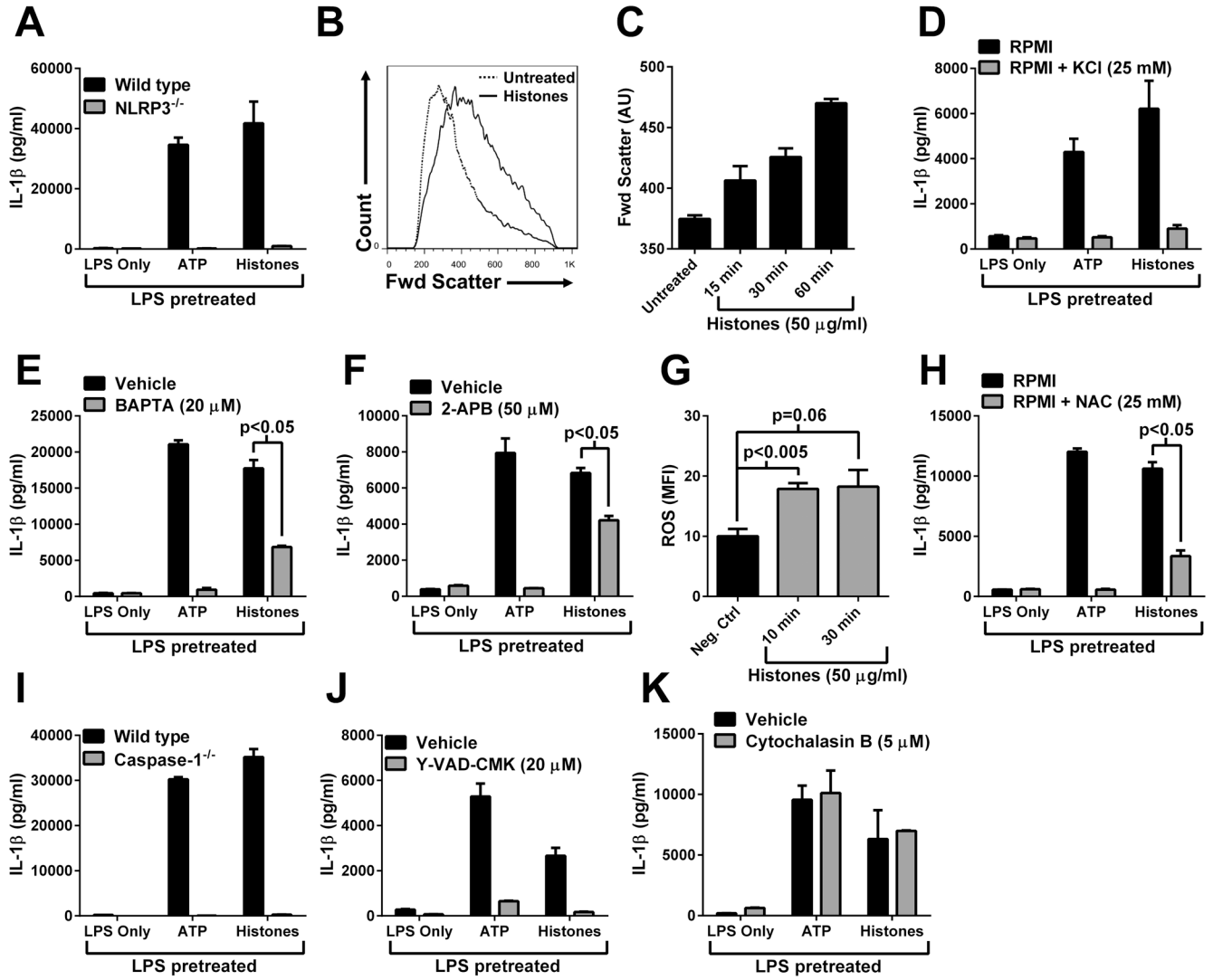
Figure 6.

Mechanism of inflammasome activation by extracellular histones. A) Macrophages were primed with LPS (100 ng/ml), then treated with ATP (1 mM) or histones (50 μg/ml). IL-1β levels in supernatants were determined by ELISA. B) Macrophages were treated with histones (50 μg/ml) for 1 hour and forward scatter (cell size) was measured by flow cytometry. C) Macrophages were analyzed as in B, at time points following histone addition. Mean forward scatter (arbitrary units, AU), representing cell swelling, was determined from $> 2 \times 10^4$ cells per sample. Results are triplicate samples representative of 2 independent experiments. D–F and H–K) Macrophages were treated as described in A. As indicated, cells were pretreated with inhibitors 15–30 min prior to ATP or histones. G) Macrophage ROS production in response to histones (n=4 mice) determined by flow cytometry (CellRox Red). Unless otherwise indicated, in vitro experiments are triplicate samples representative of 3 independent experiments.
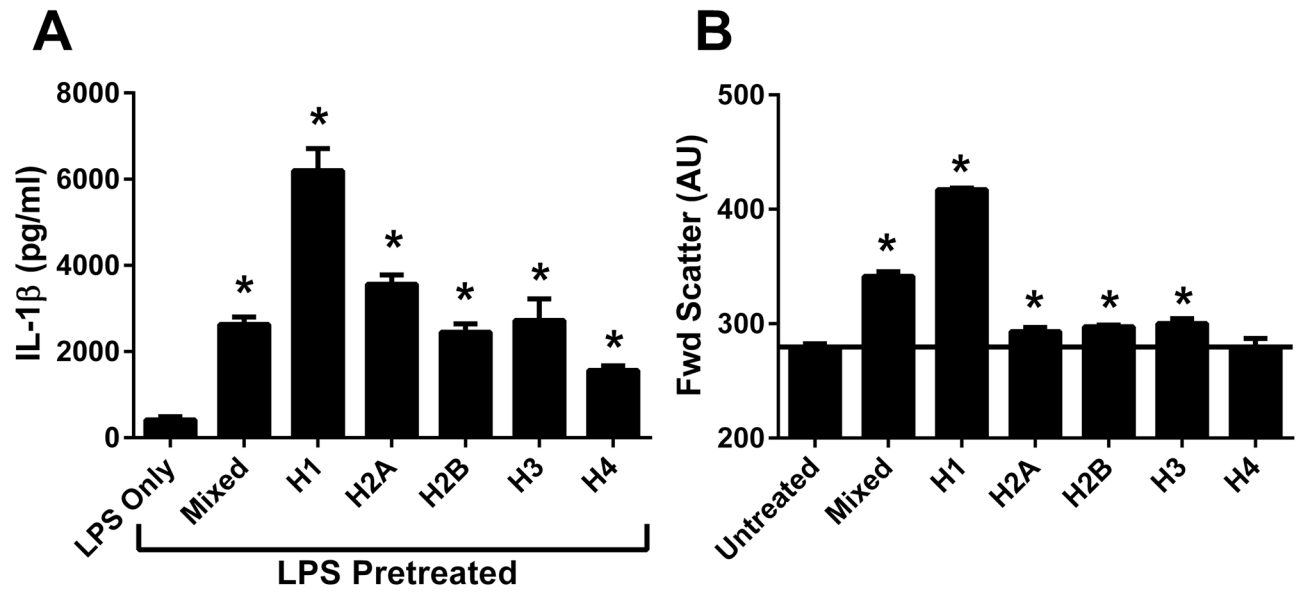
Figure 7.
Properties of individual histones. Inflammasome activation and cell swelling assays were performed as described for Fig. 6. The ability of individual histones to A) activate the inflammasome or B) induce swelling of macrophages is shown. Results are triplicate samples representative of 3 independent experiments.
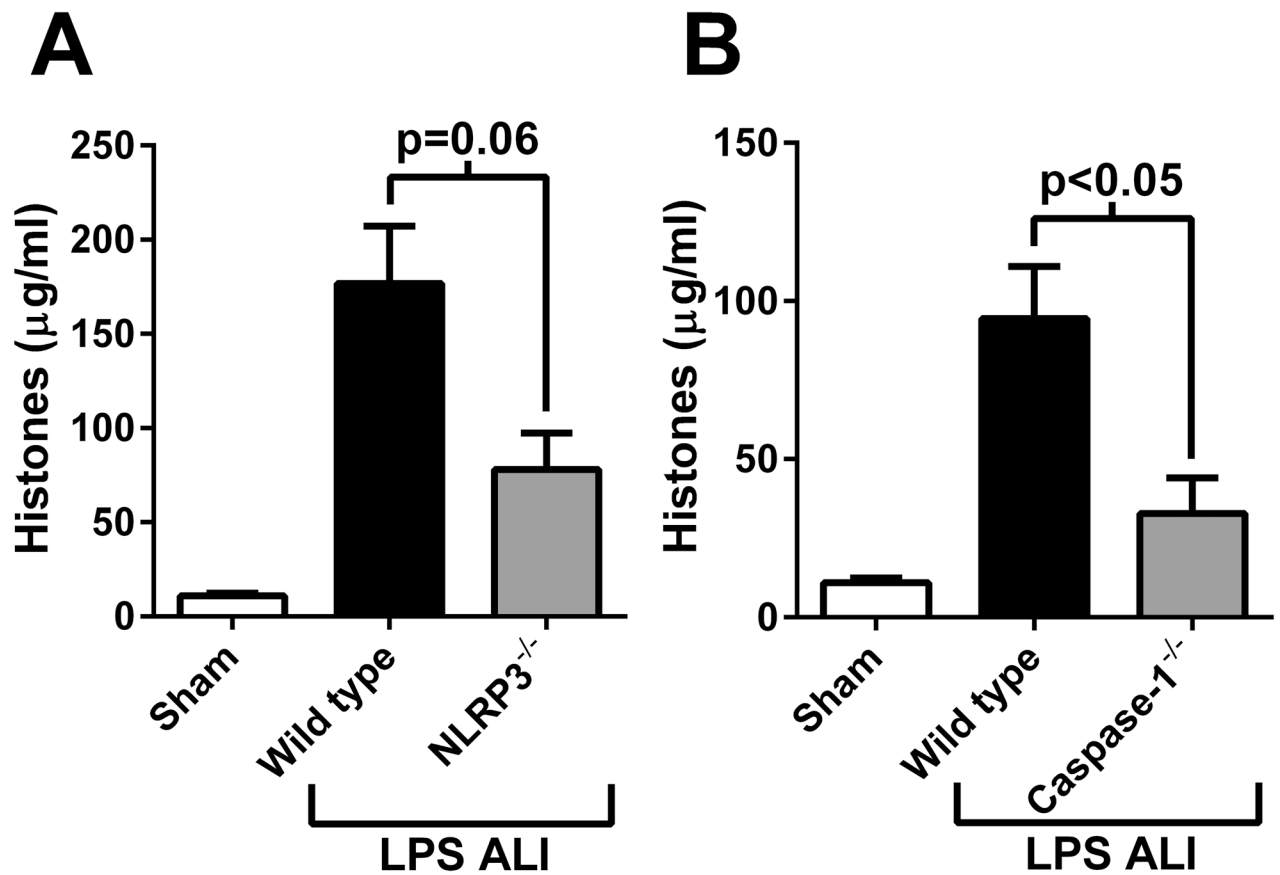
Figure 8.
The NLRP3 inflammasome is required for full extracellular histone presence during LPS-induced ALI (8 hours). A) Histone levels found in BALF from wild type or NLRP3$^{-/-}$ mice (n 5 mice per group). B) Histone levels found in BALF from wild type or caspase-1$^{-/-}$ mice (n 5 mice per group).
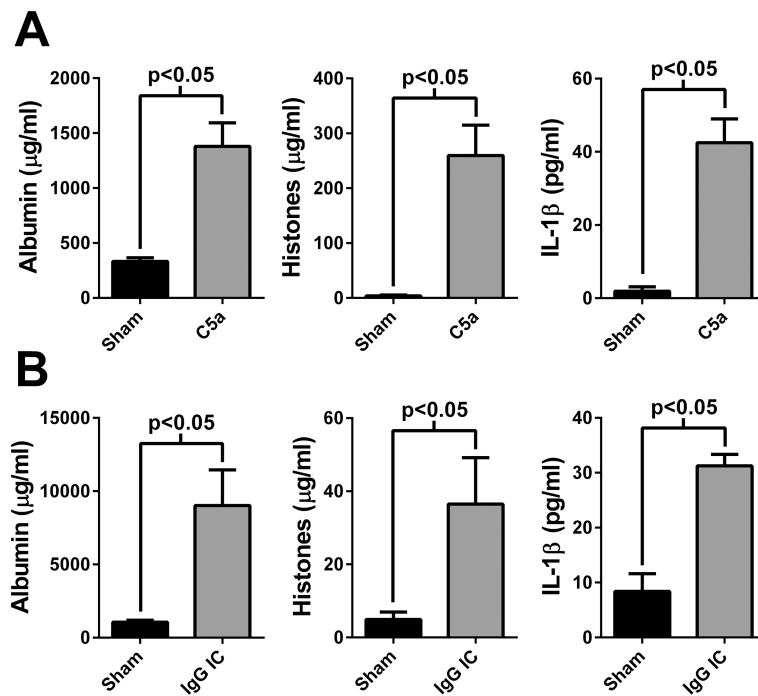
Figure 9.
Evidence that histone/inflammasome-mediated inflammation is conserved among ALI models. A) Albumin, histone, and IL-1β levels observed in BALF 6 hours after the i.t. instillation of C5a (500 ng). Sham animals received sterile PBS (n=4 mice per group). B) Albumin, histone, and IL-1β levels found in BALF 6 hours after the distal airway deposition of IgG immune complexes. Sham animals received only anti-BSA (n=5 mice per group).
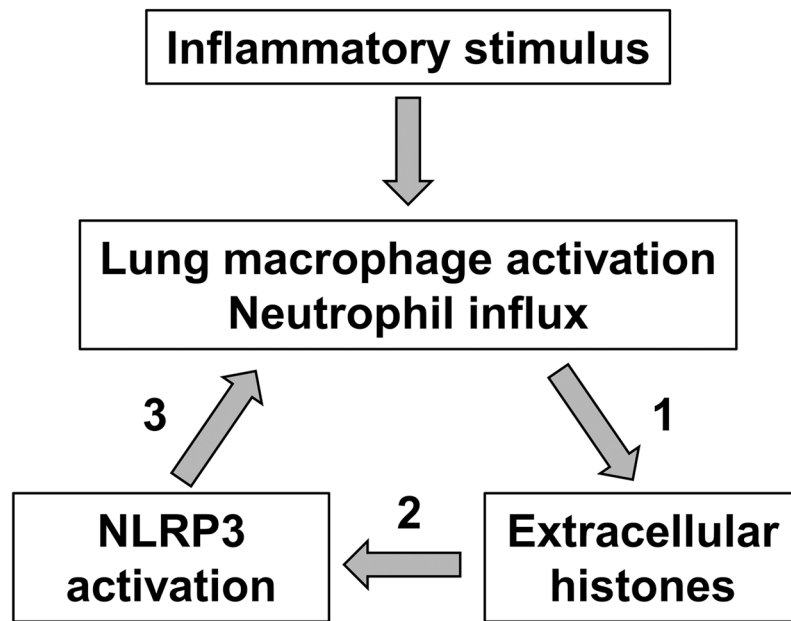
Figure 10.
Model of the interactions between extracellular histones and the NLRP3 inflammasome during ALI. 1) Neutrophils are the source of extracellular histones during ALI (Fig. 3 and 4). 2) Extracellular histones activate the NLRP3 inflammasome (Fig. 5). 3) The NLRP3 inflammasome is required for optimal neutrophil influx (Fig. 1D) and histone presence (Fig. 8).